ISSN 0083-7903, 75 (Print)
ISSN 2538-1016; 75 (Online)

Hydrology of the Bounty Islands Region

by

N.M. RIDGWAY

New Zealand Oceanographic Institute Memoir 75

1975

NEW ZEALAND

DEPARTMENT OF SCIENTIFIC AND INDUSTRIAL RESEARCH

Hydrology of the Bounty Islands Region

by

N.M. RIDGWAY

New Zealand Oceanographic Institute, Wellington

New Zealand Oceanographic Institute Memoir 75

1975

Citation according to "World List of Scientific Periodicals" (4th edn)

Mem. N.Z. oceanogr. Inst. 75

ISSN 0083 - 7903

Received for publication : January 1974

A.R. SHEARER, GOVERNMENT PRINTER, WELLINGTON, NEW ZEALAND - 1975

CONTENTS

FIGURES

TABLES

Hydrology of the Bounty Islands Region

by

N.M. Ridgway

ABSTRACT

Temperature and salinity measurements made within an area bounded by latitudes 42°S and 50°S and longitudes 178°29'E and 173°00'W are presented and discussed. The results show the influence of the Chatham Rise in determining the position of the Subtropical Convergence east of New Zealand. The surface geostrophic flow with respect to 1000 decibars is discussed and the effect of bottom topography on the flow of the Antarctic Circumpolar Current is shown. Sound velocities are calculated from the observed data, and velocity corrections for echo soundings are given and compared with those previously published.

INTRODUCTION

Between 20 January and 9 February 1969, a hydrological survey was carried out in the region of the Bounty Islands. This was the seventh and final survey of a series, carried out in successive summers, which has covered the oceanic areas around New Zealand to a distance of approximately 500 miles offshore. Previous surveys have been reported by Garner (1967a, b; 1970), Ridgway (1970), and Ridgway and Heath (1975).

In the present survey 23 serial temperature/salinity stations were successfully occupied. These stations lay in an area bounded by latitudes 42°00'S and 50°00'S, longitudes 178°29'E and 173°00'W (Stn F972 is an outlier because of bad weather). This area includes parts of such bathymetric features as the Subantarctic Slope, the Bounty Trough, the Chatham Rise, and the Hikurangi Trench. These features, and the station positions are shown in Fig. 1.

The weather throughout the cruise was frequently windy, wind speeds exceeding 5 m sec^{-1} being encountered at 12 stations (F950-952, 956, 958, 960, 963, 965, 968-971). Station circumstances are described in Table 1.

Data were collected and analysed using the same equipment and techniques as described in the reports of previous surveys (*see*, e.g., Ridgway 1970 : 8-9).

The observed values of temperature and salinity at stated sampling depths, computed values of density, sound velocity, and dynamic height anomaly are listed in the Appendix.

New Zealand Oceanographic Institute Memoir 75. 1975. 27 p.
ISSN 0093-7903.

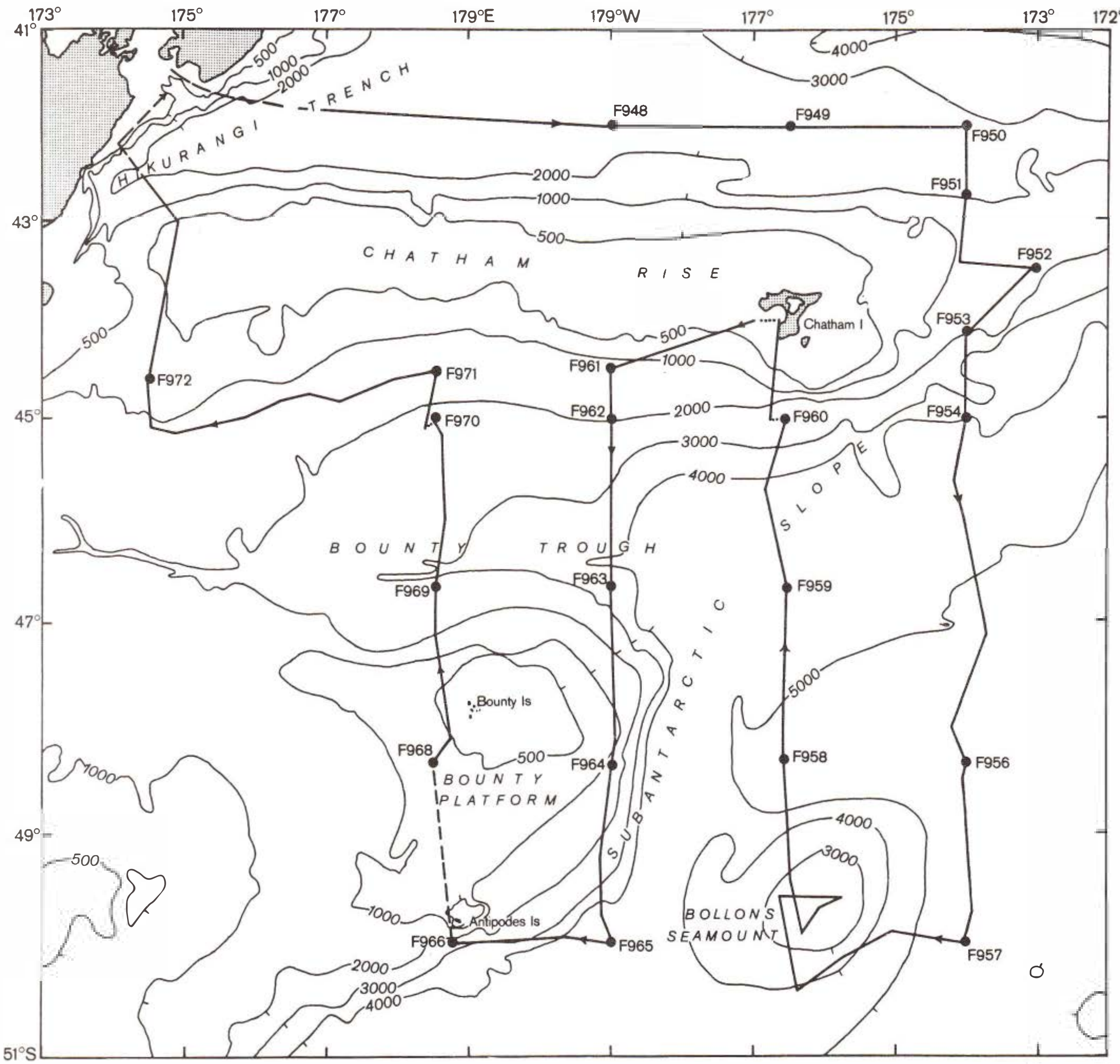

Fig. 1. The survey area showing station positions and bathymetric features. Isobaths are shown in metres.

DISCUSSION

Subtropical Convergence

One of the main hydrological features in New Zealand's waters is the Subtropical Convergence which separates Subantarctic Water from Subtropical Water. It is usually marked by a steep horizontal gradient in the surface salinity, any corresponding surface temperature gradient being much less pronounced. Garner (1962 : 15) pointed out that the surface properties depend, in part, on climate to which salinity is much less sensitive than temperature.

According to Burling (1961 : 26), the convergence east of New Zealand occupies a narrow band of latitude marked by surface salinity values of between 35.0 and 34.5‰. Deacon (1937) concluded that surface water north of the 14.5°C isotherm in summer and the 11.5°C isotherm in winter belongs to the Subtropical Water mass, whereas Garner (1959) stated

TABLE 1

STATION CIRCUMSTANCES

Air (screen) temperatures measured and wind properties estimated at bridge level.

NZOI Stn No.	N.Z. DATE / TIME (Jan.-Feb. 1969) Start	Finish	STATION POSITION Latitude (°S)	Longitude	Bottom Depth (m)	Air Temp. (°C)	WIND Direct-ion (°T)	Speed m sec⁻¹
F948	20/2220	20/0030	42 00'	179 00'W	2500	18.6	300	4.1
F949	21/1120	21/1310	42 00'	176 30'W	2800	19.5	350	3.1
F950	22/0010	22/0415	42 00'	174 00'W	2900	18.4	000	6.2
F951	22/1015	22/1445	42 43'	174 00'W	2100	18.9	340	9.3
F952	23/0015	23/0200	43 30'	173 00'W	1750	15.4	260	6.7
F953	23/1152	23/1443	44 15'	174 00'W	2700	15.1	250	1.5
F954	23/2037	23/2335	45 00'	174 00'W	3200	14.5	180	3.1
F956	25/0610	25/0943	48 20'	174 00'W	5200	10.5	240	5.1
F957	25/2154	26/0106	50 00'	174 00'W	5200	11.0	310	3.1
F958	28/0252	28/0905	48 18'	176 33'W	4900	11.5	190	6.2
F959	28/2010	29/0020	46 40'	176 30'W	4600	12.5	LIGHT AIRS	
F960	29/1227	29/1540	45 00'	176 30'W	1800	15.0	010	7.2
F961	31/0635	31/0803	44 30'	179 00'W	900	16.0	010	3.6
F962	31/1108	31/1235	45 00'	179 00'W	1900	16.9	000	3.1
F963	31/2152	1/0235	46 40'	179 00'W	4000	15.5	000	5.1
F964	1/1138	1/1450	48 20'	179 00'W	1450	12.7	220	4.6
F965	2/0236	2/0750	50 00'	179 00'W	4400	10.0	270	6.2
F966	3/2310	3/0130	50 00'	178 45'E	3400	9.5	290	1.5
F968	4/0926	4/1027	48 20'	178 29'E	700	11.5	220	9.3
F969	4/2250	5/0135	46 40'	178 30'E	2600	12.6	220	7.7
F970	5/1340	5/1522	45 00'	178 30'E	2500	16.5	000	10.2
F971	5/2130	5/2334	44 30'	178 30'E	1350	15.4	200	7.7
F972	8/0430	8/0600	44 36'	174 30'E	800	11.2	180	2.6

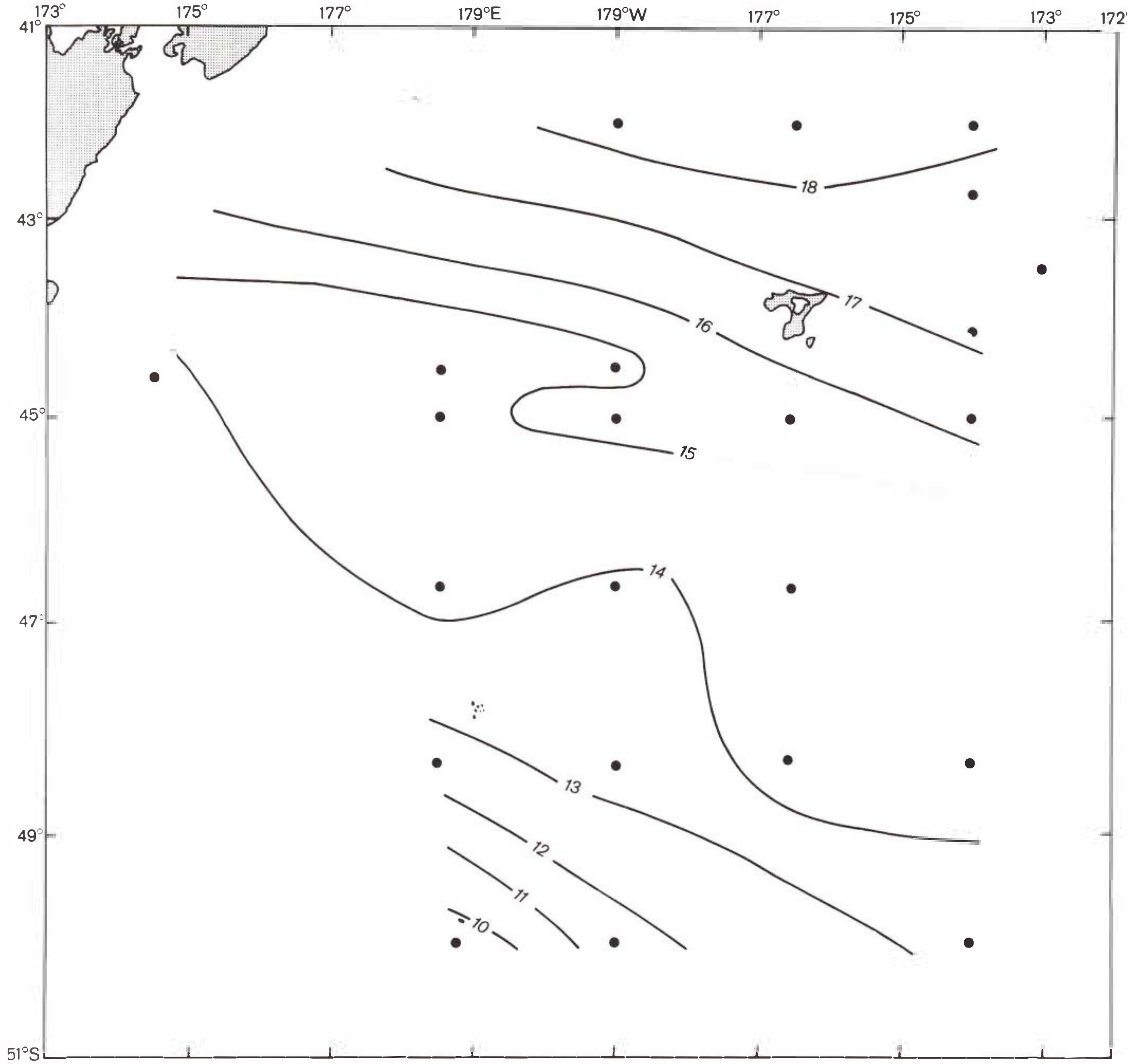

Fig. 2. Isotherms (°C) at the sea surface.

that the convergence follows approximately the 15°C surface isotherm in February, the 10°C surface isotherm in August, and the 34.7 to 34.8‰ surface isohaline with little seasonal variation.

Heath (1975) has suggested that, east of New Zealand, the Chatham Rise limits the southward movement of the convergence, since it provides a physical barrier to the movement of water at depths below that of the Rise. Water above this depth is limited in its southward movement by frictional coupling with the water below.

Surface isotherms and isohalines drawn from data obtained during the present survey are shown in Figs 2 and 3 respectively. Surface temperatures ranged between 10°C in the south and 18°C in the north. No steep surface temperature gradients existed, but the gradient between 10°C and 12°C was steeper than elsewhere (Fig. 2). Surface salinities ranged between 34.2‰ in the south and 35.5‰ in the north (Fig. 3). A relatively steep horizontal salinity gradient existed between the 34.4 and 35.5‰ isohalines, particularly west of the Chatham Islands. East of the islands the 34.3 to 34.9‰ isohalines trended southwards.

The distribution of temperature and salinity at a depth of 200 m is shown in Figs 4 and 5 respectively. (Values at this depth would be less responsive to climatic variations than those at the surface.) Temperatures at this depth (Fig. 4) varied between 6°C in the south to almost 14°C in the north and were, in general, about 4°C lower than the surface temperatures. A relatively steep temperature gradient between 8 and 13°C was present west of the Chatham Islands and, east of the islands, the 9 to 11°C isotherms trended towards the south.

Salinities at 200 m ranged from 34.8‰ in the south to 35.2‰ in the north (Fig. 5). A relatively steep horizontal salinity gradient between 34.5 and 35.2‰ was present west of the Chatham Islands and, east of the islands the 34.6 to 34.9‰ isohalines trended southwards (Fig. 5). The relatively steep horizontal gradients of temperature at a depth of 200 m (Fig. 4) and of salinity, both at the surface (Fig. 3) and at 200 m (Fig. 5) may all be taken as representing the Subtropical Convergence region. The gradients may have been locally steeper than those shown in the

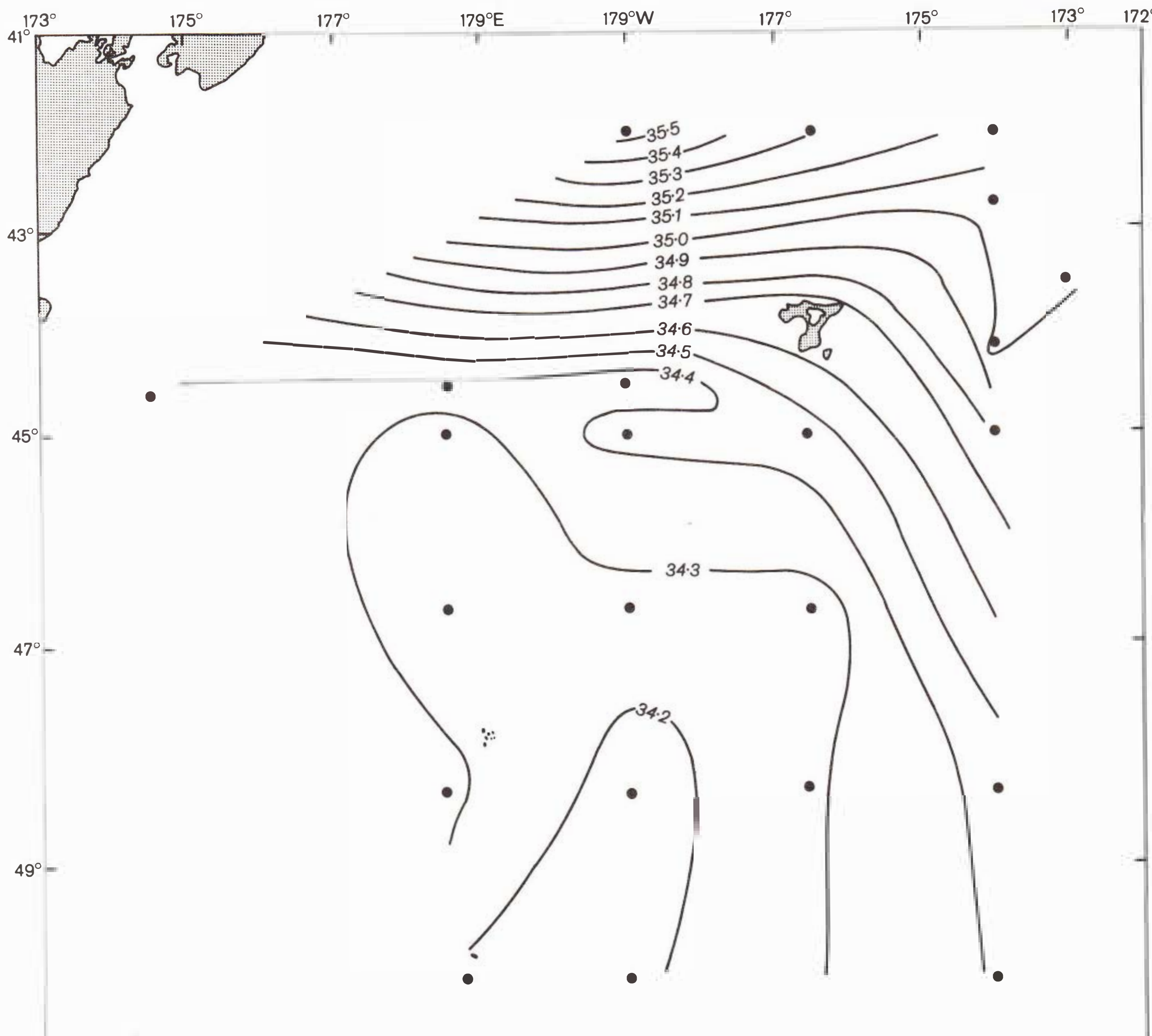

Fig. 3. Isohalines (‰) at the sea surface.

figures, because the distance between the northernmost zonal line of stations and those in the next line south was at least 280 km. The southward trend of the isolines to the east of Chatham Islands supports Heath's (1975) contention that the Chatham Rise controls the position of the Subtropical Convergence.

The more southerly position of the Subtropical Convergence to the east of the Chatham Islands is further illustrated in the longitudinal cross-sections of salinity shown in Figs 6 and 7. A sub-surface tongue of more saline water (>34.4‰) extended southwards in both sections. Along about longitude 179°W (Fig. 6) this sub-surface tongue (represented by the 34.4‰ isohaline) extended to just south of latitude 45°S (Stn F962), whereas along about longitude 174°W (Fig. 7) it extended south of latitude 50°S (Stn F957).

The position of the Subtropical Convergence is not clearly defined in the corresponding temperature cross-sections (Figs 8 and 9), although in the section

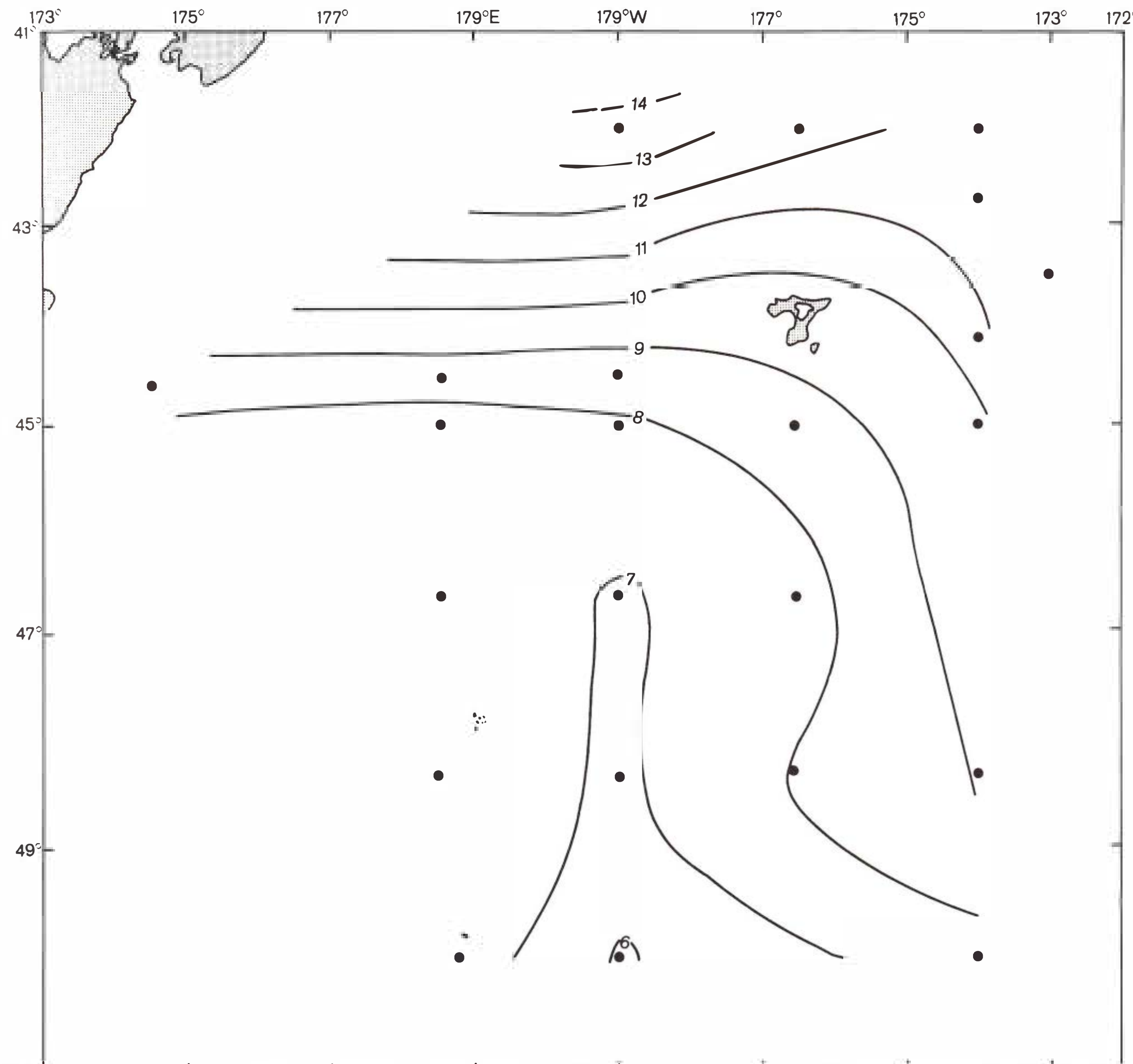

Fig. 4. Isotherms (°C) at a depth of 200 m.

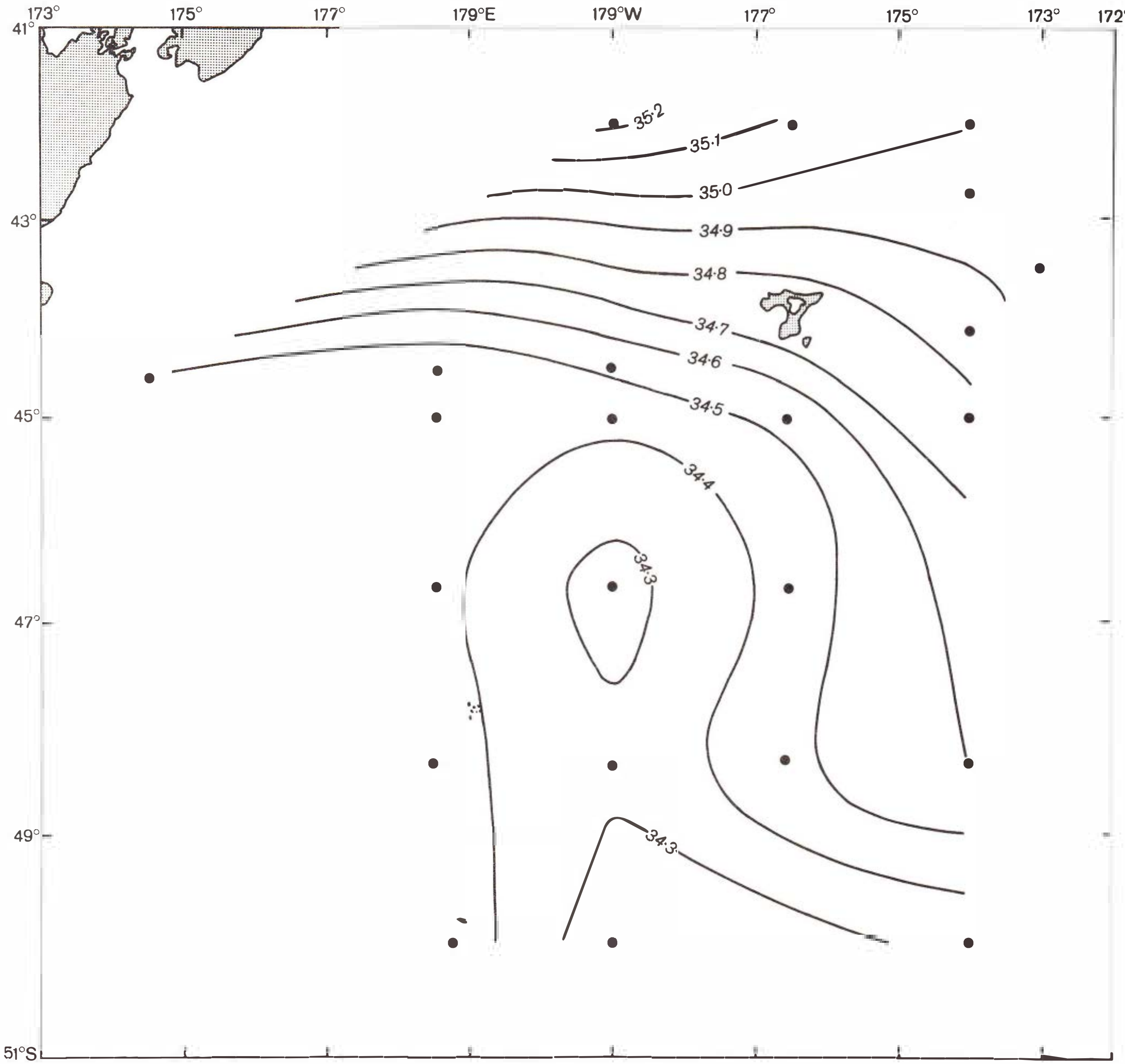

Fig. 5. Isohalines (‰) at a depth of 200 m.

along about longitude 179°W (Fig. 8) a well-developed thermocline, at depths between 30 and 70 m, extended southwards from Stn F961. The 9°C isotherm marked the bottom of this thermocline. North of Stn F961 this thermocline weakened and the near-surface isotherms sloped down towards the north. In the section along about 174°W (Fig. 9) a thermocline, marked at the bottom by the 12°C isotherm, extended over the entire length of the section. Warmer surface water extended further southwards in this section than in the previous one (Fig. 8) because the Subtropical Convergence lies further southwards east of the Chatham Islands and Subtropical Water lies to the north of this convergence.

Further evidence of the position of the Subtropical Convergence is provided by the geopotential topographic contours of the sea surface relative to 200 decibars (Fig. 10). These contours represent the surface geostrophic flow relative to the flow at a depth of approximately 200 m. North of about latitude 45°S, the dynamic height anomalies varied between 31 and 37 dynamic centimetres (dyn. cm) and the surface geostrophic flow was directed eastwards. A second

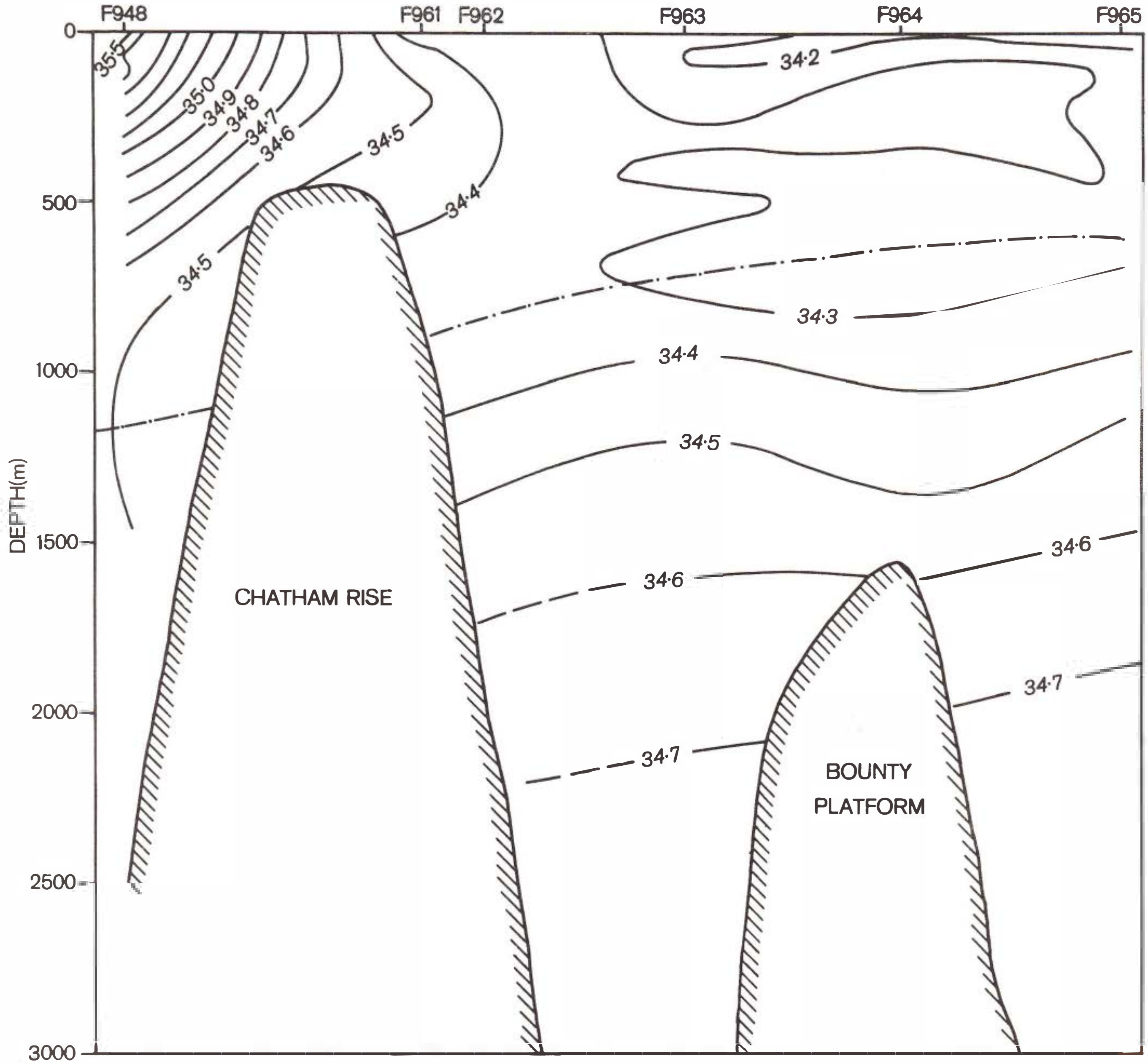

Fig. 6. Vertical cross-section of salinity (‰) along approximate longitude 179°W. Station numbers are shown. Dashed line indicates the depth of the core of minimum salinity water.

31 dyn. cm contour, just south of latitude 45°S, was separated from the northernmost 31 dyn. cm contour by a slight trough in the sea surface elevation. The flow along the southern edge of this trough was westwards east of this longitude.

Using the region between the two 31 dyn. cm contours as defining the Subtropical Convergence, the position of the convergence during the period of the survey is illustrated in Fig. 11. Also shown in this figure is the position of the convergence as defined in the longitudinal cross-sections by the southward extent of the sub-surface tongues of more saline water. Both the geopotential topographic contours and the salinity at 200 m, relying on sub-surface properties, give similar positions for the Subtropical Convergence. For comparison, the positions of the convergence using the surface salinity values defined by Garner (1959) and Burling (1961) are given on the same figure. All positions of the Subtropical Convergence in Fig. 11 show that it parallels lines of latitude west of, and trends southwards to the east of, the Chatham Islands.

Geostrophic Circulation

The surface geostrophic flow relative to the 1000 decibar surface is shown by the dynamic height anomaly contours in Fig. 12. Anomaly values of 1.3 to 1.4 dynamic metres (dyn. m) were found north of the Chatham Islands. Previous results (Garner 1969; Heath 1972) have shown that the 1.4 dyn.m contour east of the North Island generally defines the movement of the East Cape Current.

Garner (1969: *see* fig. 3 and p.216) also showed that values less than 1.1 dyn. m indicated the Antarctic Circumpolar Current. Although generally eastwards flowing, this current flows southwards around the western margin of the Campbell Plateau south of New Zealand. The present results indicate that this current then flows north-eastwards along the eastern flank of the plateau and, upon approaching the Chatham Rise, turns in a clockwise direction to flow south-eastwards. These results confirm and extend those of Garner

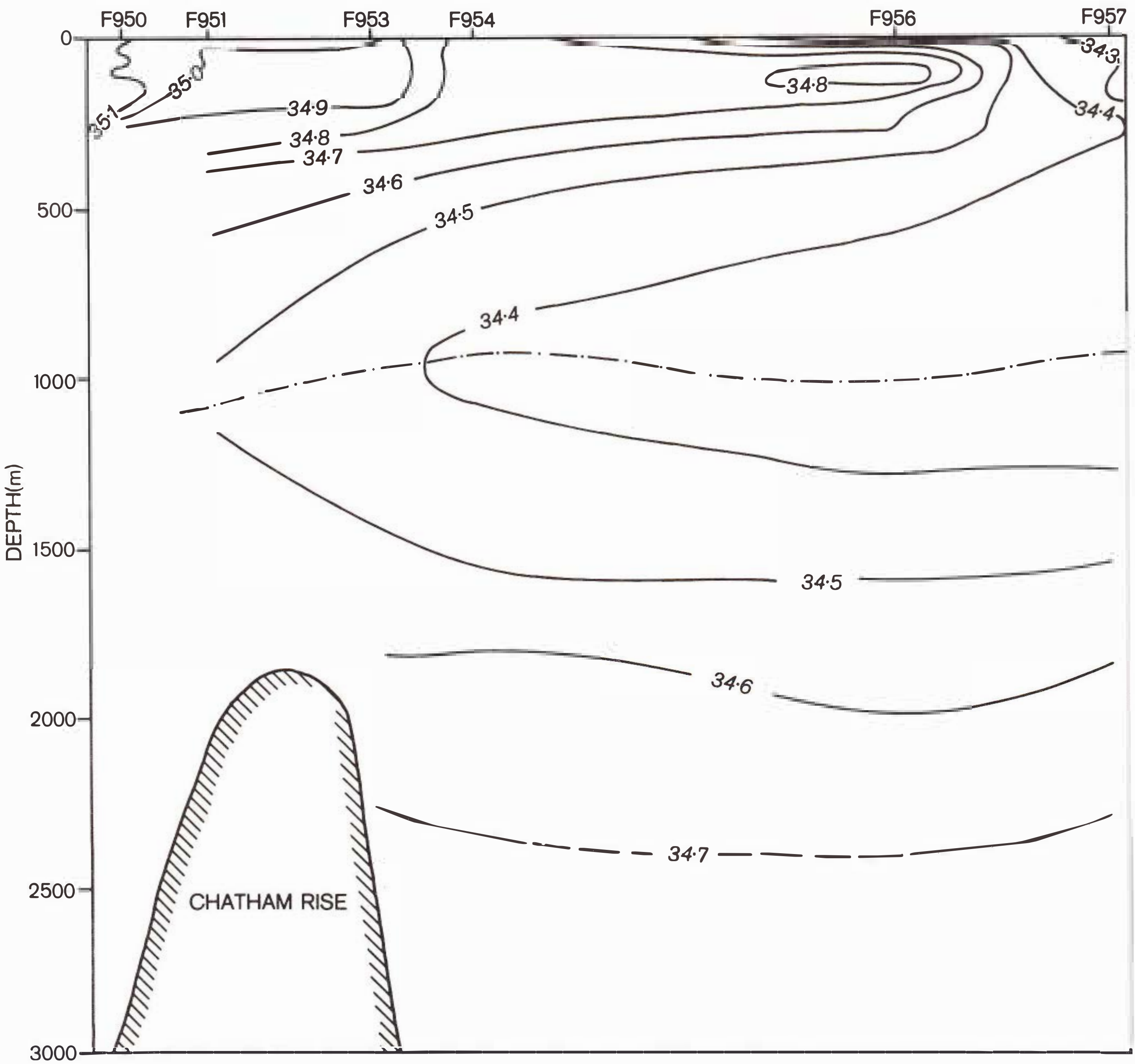

Fig. 7. Vertical cross-section of salinity (‰) along approximate longitude 174°W. Station numbers are shown. Dashed line indicates the depth of the core of minimum salinity water.

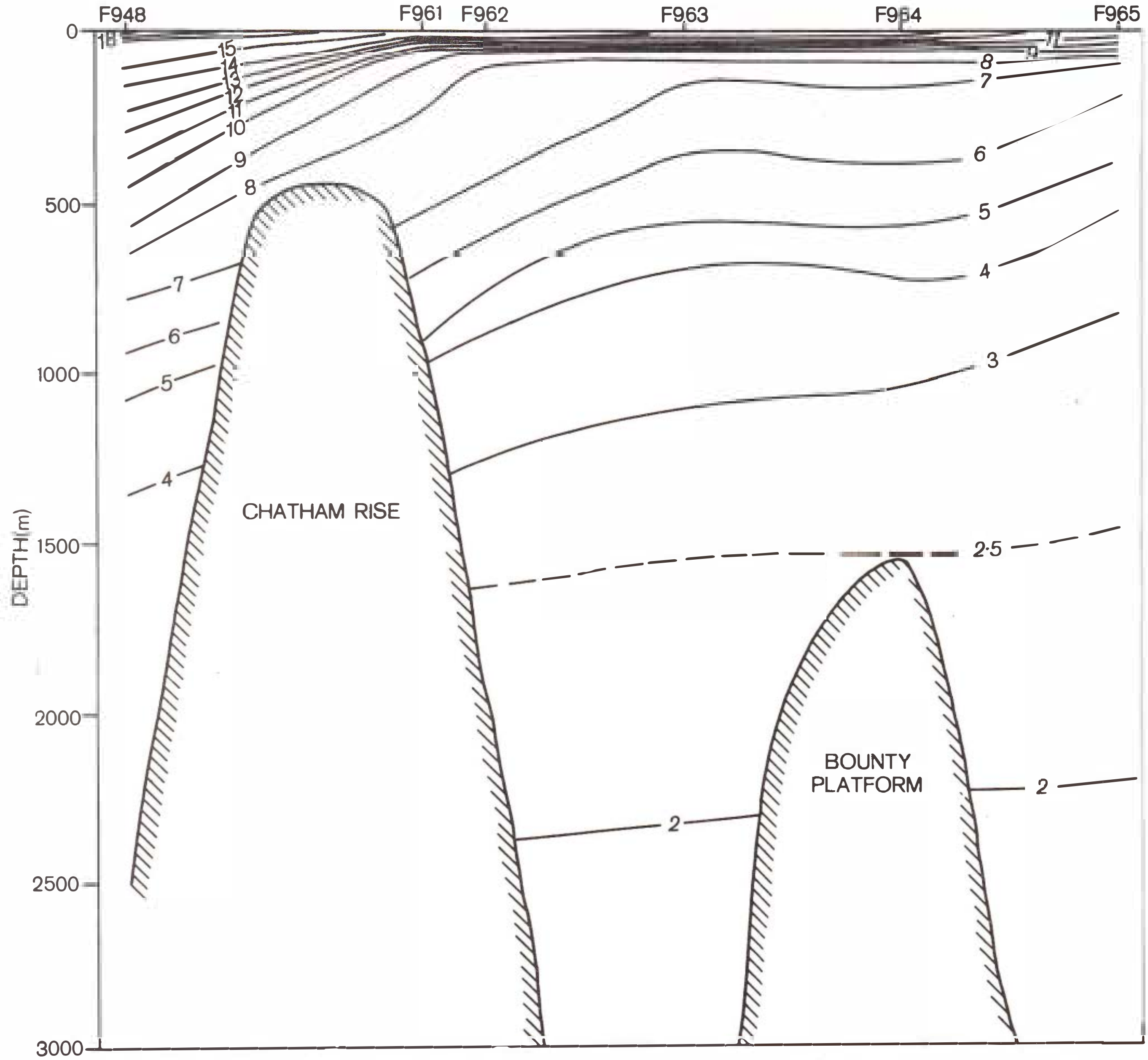

Fig. 8. Vertical cross-section of temperature (°C) along approximate longitude 179°W. Station numbers are shown.

who described a valley in the surface geopotential topography which reached over the Bounty Trough. He also noted the south-eastwards trend of the streamlines south of the Chatham Islands and suggested that a planetary wave system is induced in the zonal flow of the Circumpolar Current by the topography of the Campbell Plateau. The present results also indicate the effect of the Chatham Rise in turning the flow towards the southeast.

ANTARCTIC INTERMEDIATE WATER

Isohalines of the minimum salinity which marks the core of Antarctic Intermediate Water are shown in Fig. 13 and isobaths of the core depth are shown in Fig. 14.

Salinity increased from less than 34.25‰ in the south-west to more than 34.45‰ in the north-east,

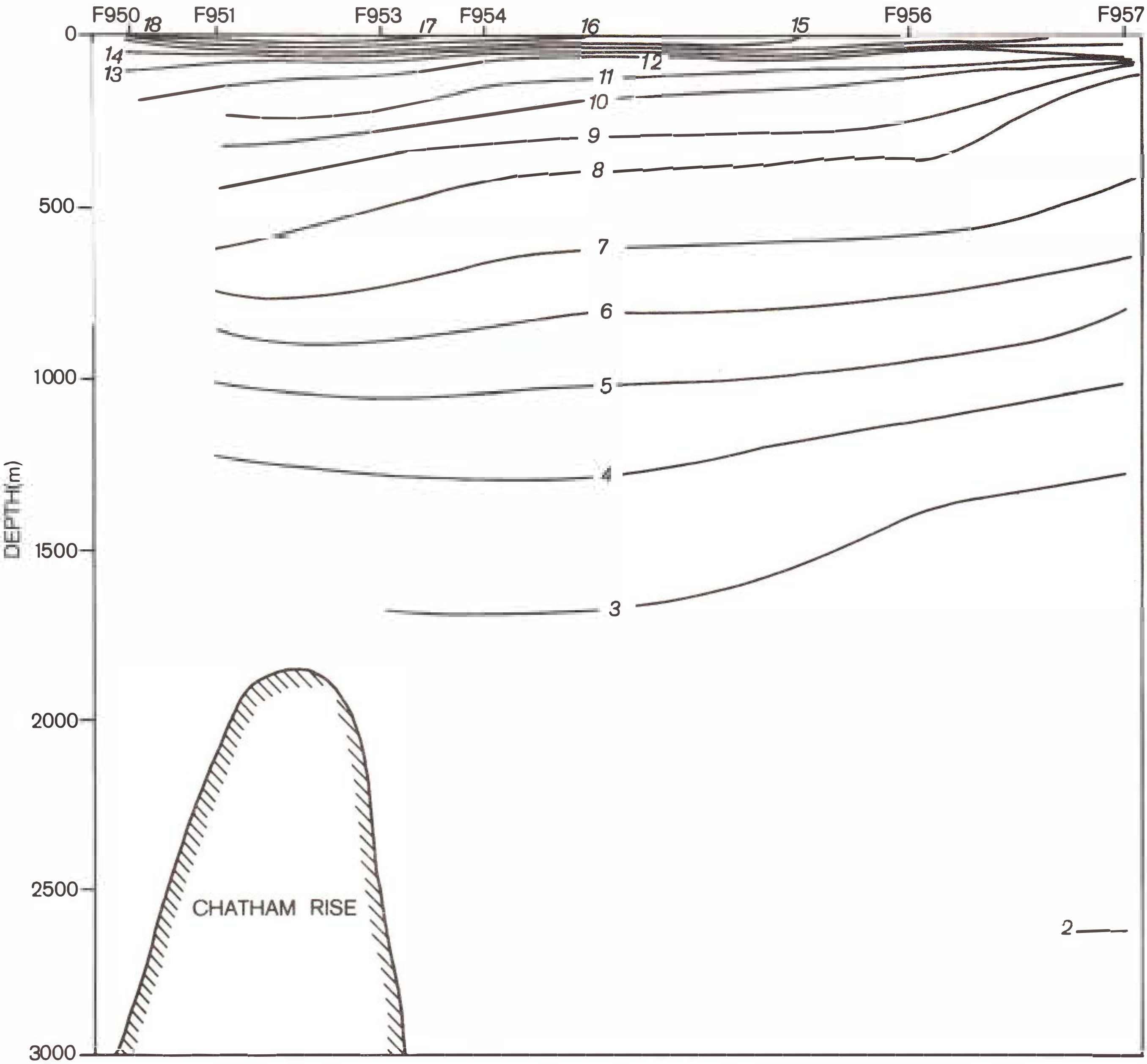

Fig. 9. Vertical cross-section of temperature (°C) along approximate longitude 174°W. Station numbers are shown.

tongue-like features being indicated by the 34.25 and 34.3‰ isohalines (Fig. 11). As Antarctic Intermediate Water (formed at the Antarctic Convergence) moves towards lower latitudes its salinity increases by mixing with more saline water from above and below. The results obtained may therefore be interpreted as indicating a general spreading of Antarctic Intermediate Water towards the north-east. The increase in salinity was accompanied by an increase in the core depth, from less than 600 m in the south-west to over 1000 m in the north-east of the survey area (Fig. 14).

Deep Water

Deep Water, which lies below Antarctic Intermediate Water, is marked by a salinity maximum at 2500 to 3000 m in the region east of the Campbell

Fig. 10. Geopotential topography of the sea surface relative to 200 dbar. Values are in dynamic centimetres. Arrows show the direction of the relative geostrophic flow.

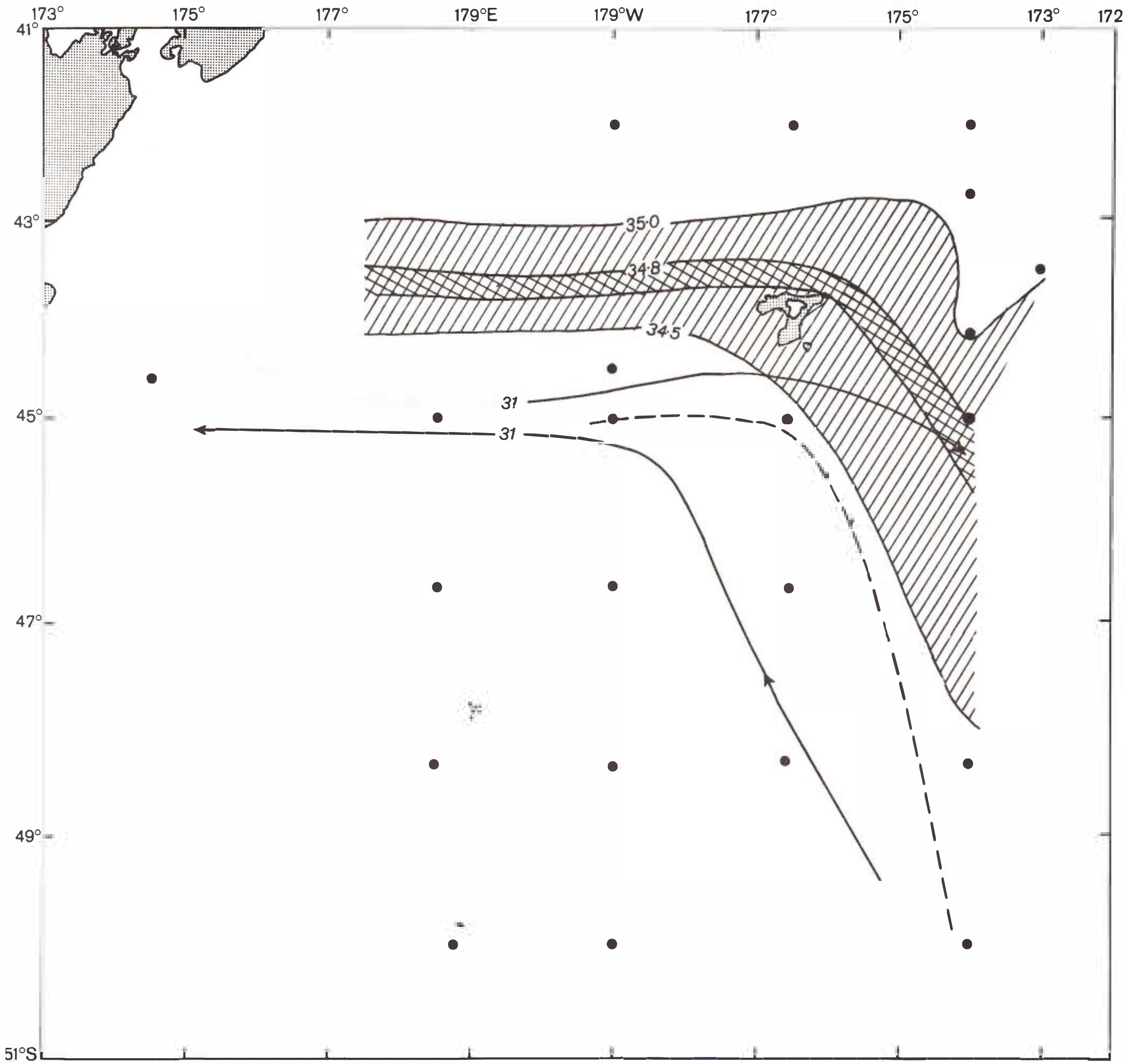

Fig. 11. Position of the Subtropical Convergence as defined by - (a) the 31 dyn. cm contours (0/200 dbar, solid lines), arrows show the direction of the relative geostrophic flow; (b) the southward extent of sub-surface water with a salinity of 34.4‰ (dashed lines); (c) surface salinity values defined by Garner (1959) (light shading); (d) surface salinity values defined by Burling (1961) (heavy shading).

Plateau although, north of about 40°S, the highest salinities below the Antarctic Intermediate Water are found in the bottom water of the Pacific Ocean (Neumann and Pierson 1966 : 478).

At Stn F957, where observations extended to a depth of 3343 m, a slight salinity maximum of 34.73‰ was found at a depth of 2854 m. At Stn F958 observations extended to 2863 m, and a maximum salinity of 34.74‰ was found at this depth.

Observations at other stations did not extend sufficiently deep to indicate the presence of Deep Water.

Sound Velocity

Sound velocities derived from the observed data were computed using the formula given by Wilson (1960) and are shown in the Appendix. These sound

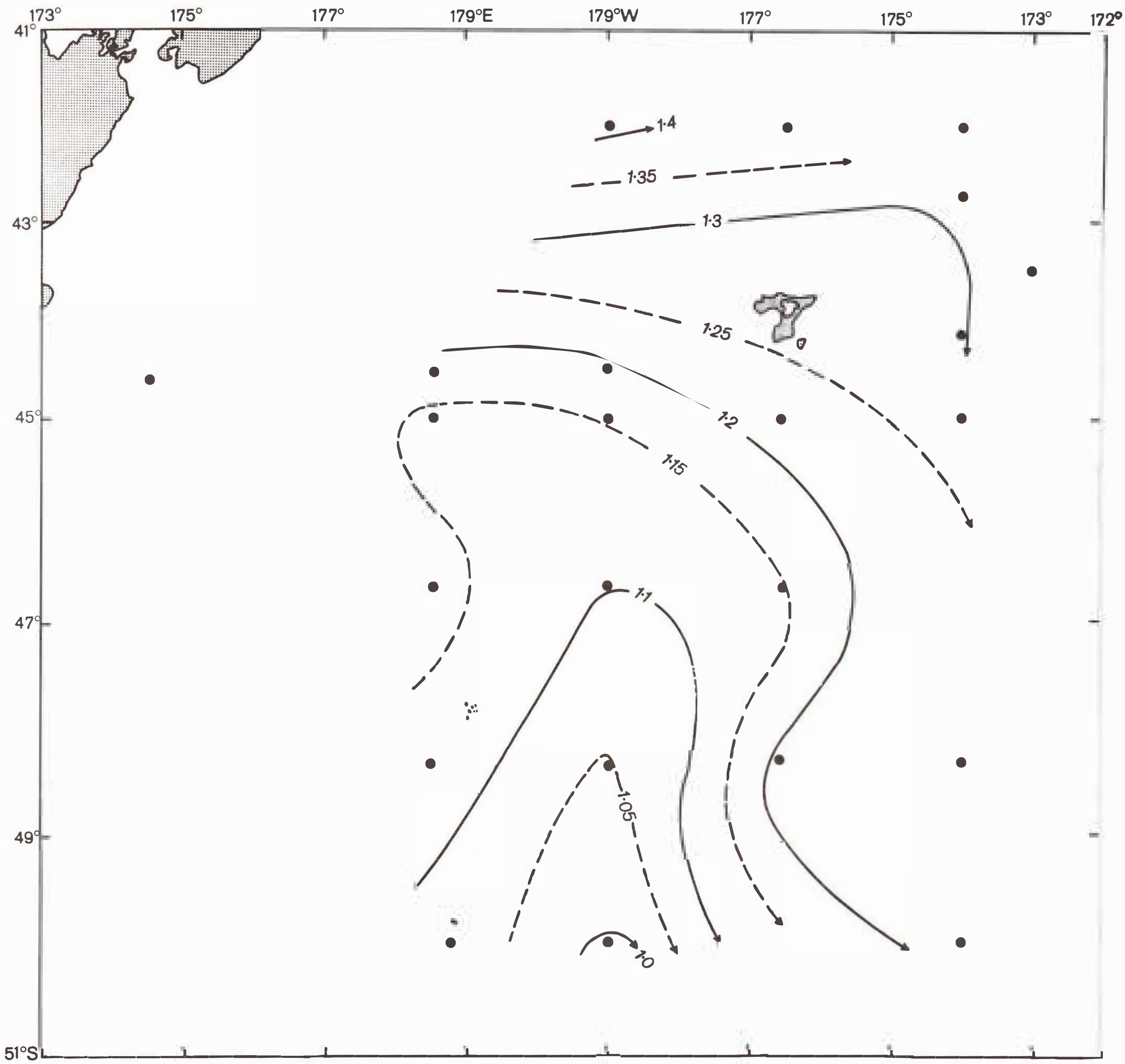

Fig. 12. Geopotential topography of the sea surface relative to 1000 dbar. Values are in dynamic metres. Arrows show the direction of the relative geostrophic flow.

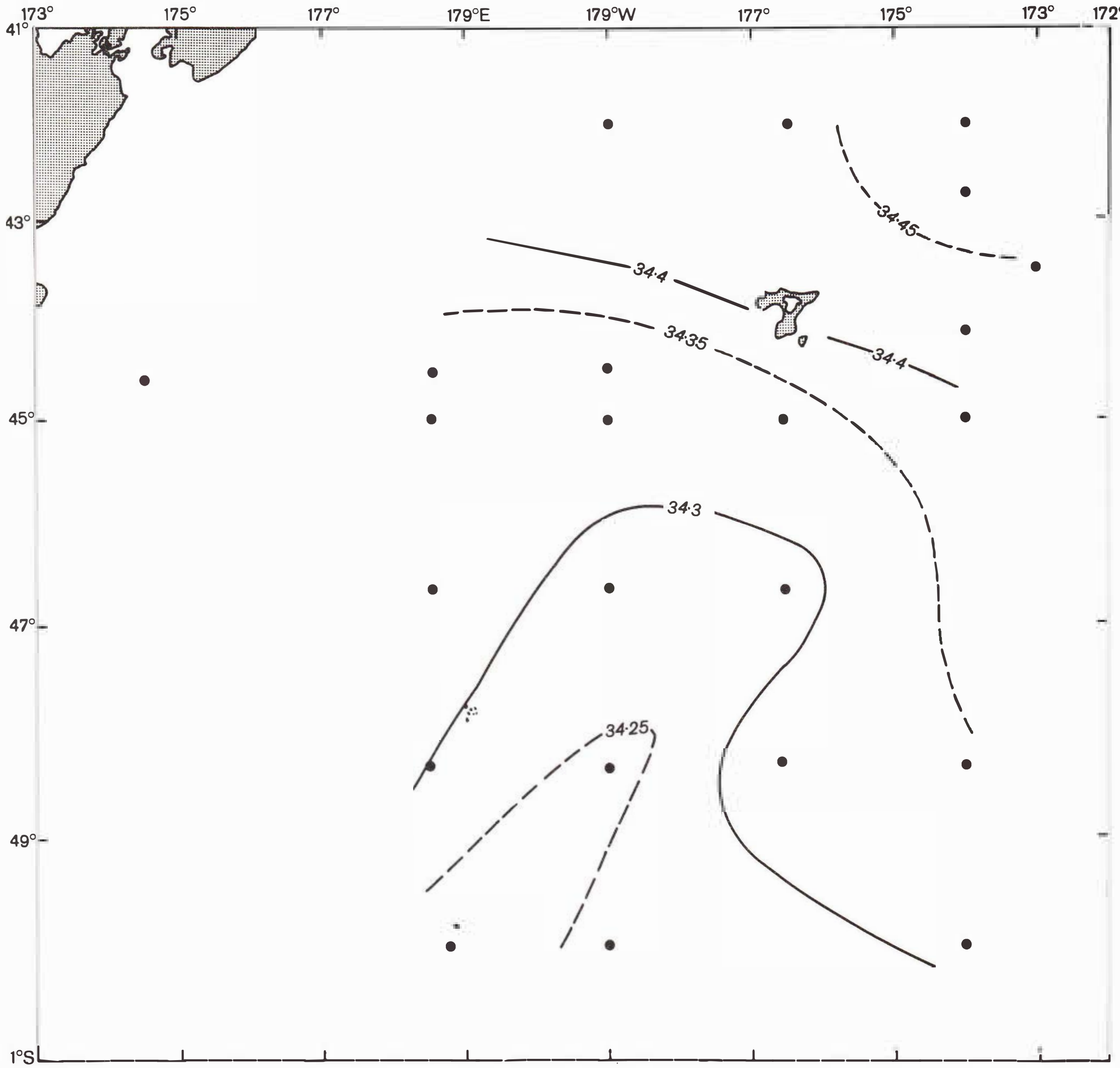

Fig. 13. Isohalines (‰) of the minimum salinity marking the core of Antarctic Intermediate Water.

velocities values supplement the work of Garner (1967c), who described the general configuration of major sound channels around New Zealand. A meridional cross-section showing the vertical distribution of sound velocity is plotted in Fig. 15. This cross-section coincides with the cross-sections of temperature and salinity shown in Figs 9 and 7 respectively.

Minimum values of sound velocity marking the SOFAR channel were present at all the deep stations shown in the section, the axis of the channel lying at a depth of approximately 1250m. At Stn F957 a second velocity minimum was present, with its axis at a depth of between 200 and 300m. This minimum marks the "Subantarctic duct" described by Garner (1967c). At all stations in the survey area which were sufficiently deep, minimum velocities marking the

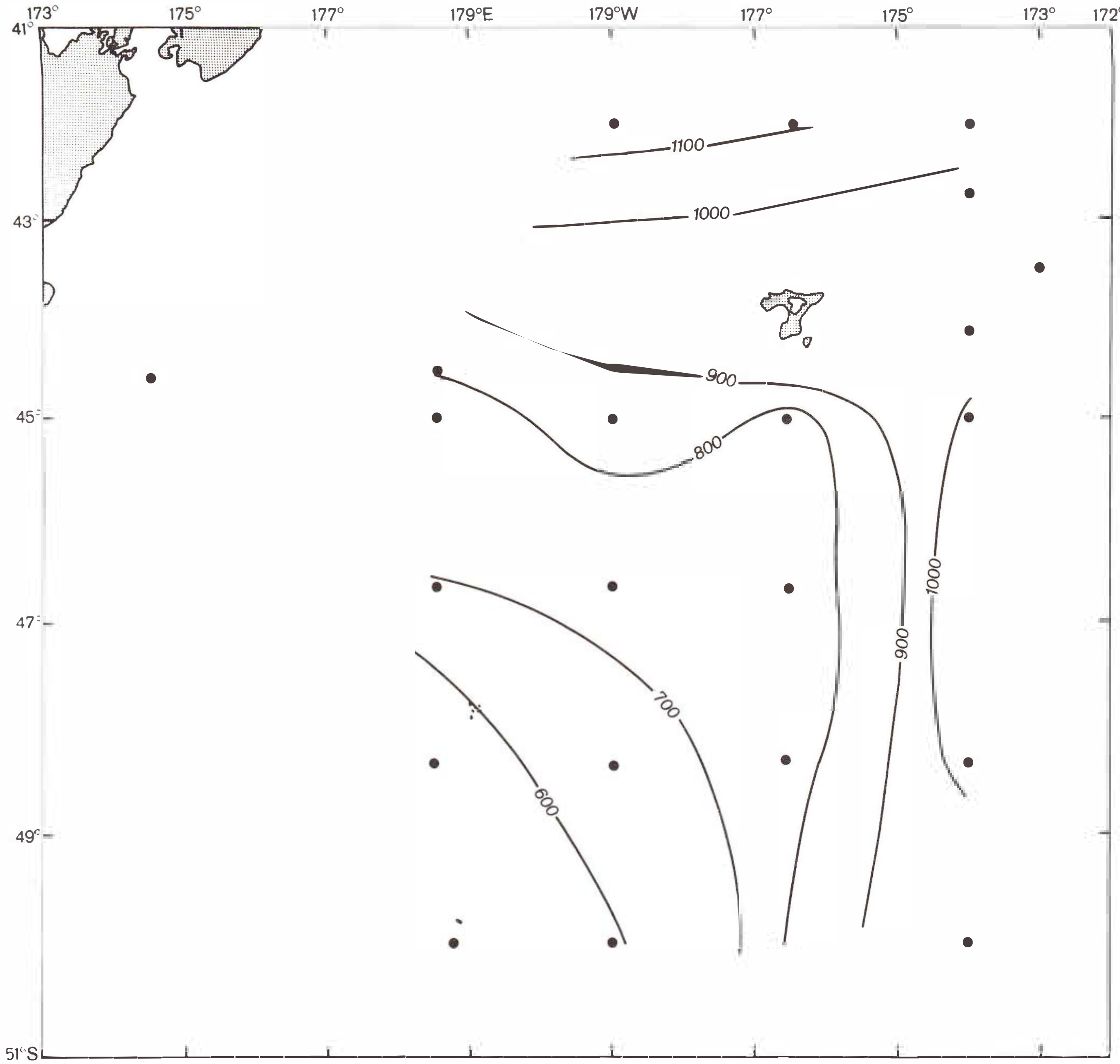

Fig. 14. Isobaths (m) of the depth of the core of Antarctic Intermediate Water.

SOFAR channel could be detected. These minimum velocities ranged between 1488.7 m sec^{-1} (Stn F948) and 1475.2 m sec^{-1} (Stn F965) and were found at depths of between 608 m (Stn F971) and 1298 m (Stn F949).

Secondary minimum velocities which may be associated with the subantarctic duct were found at all stations south of the Chatham Islands with the exception of Stns F953, 954, 956, 965, and 968. These minimum velocities varied between 1497.7 m sec^{-1} (Stn F963) and 1487.1 m sec^{-1} (Stn F972) and were located at depths of between 128 m (Stn F969) and 365 m (Stn F971).

The velocity and depth values quoted above were taken directly from the data given in the Appendix. Because of the spacing of the sampling depths, it is unlikely that the true minimum velocities in the water column were detected.

TABLE 2

ECHO SOUNDING CORRECTIONS

Corrections (m) to be added to echo soundings obtained from machines calibrated at 1500 m sec^{-1} derived from data given in the Appendix. Corrections are shown for three stations together with the appropriate area corrections from Matthews Tables.

Depth (m)	Stn F959	Matthews Area 23	Stn F966	Matthews Area 24	Stn F953	Matthews Area 43
200	-2	-2	-2	-4	0	-1
400	-4	-6	-5	-7	-1	-3
600	-6	-9	-7	-11	-2	-6
800	-9	-11	-10	-14	-3	-7
1000	-11	-13	-13	-18	-5	-9
1200	-14	-16	-16	-21	-6	-12
1400	-16	-19	-18	-23	-8	-14
1600	-18	-20	-20	-26	-9	-16
1800	-20	-23	-22	-28	-10	-18
2000	-21	-24	-23	-28	-11	-20
2200	-22	-25			-12	-21
2400	-22	-26				
2600	-23	-26				
2800	-22	-26				
3000	-22	-26				

ECHO SOUNDING CORRECTIONS

As in previous surveys of this series, the corrections to be applied to echo sounders calibrated for a speed of sound of 1500 m sec^{-1} are given in the Appendix. Errors which may arise using this assumed speed are generally corrected with tables prepared by Matthews (1939) for the British Admiralty. He divided the oceans into 52 areas, shown on charts provided with the tables, and gave corrections for each of these areas. Three of his areas (Nos 23, 24, 43) are included in the survey area discussed here; and in Table 2 the corrections calculated from data collected at one station in each area are compared with the corrections supplied by Matthews.

The corrections derived from the station data (determined from the integrated mean sounding velocity between the sea surface and each sampling depth) are generally smaller than those given in Matthews' tables. This confirms the trend in previous surveys of this series (Garner 1967a, 1967b, 1970; Ridgway 1970; Ridgway and Heath 1975) and suggests the desirability of a revision of Matthews' tables for this area.

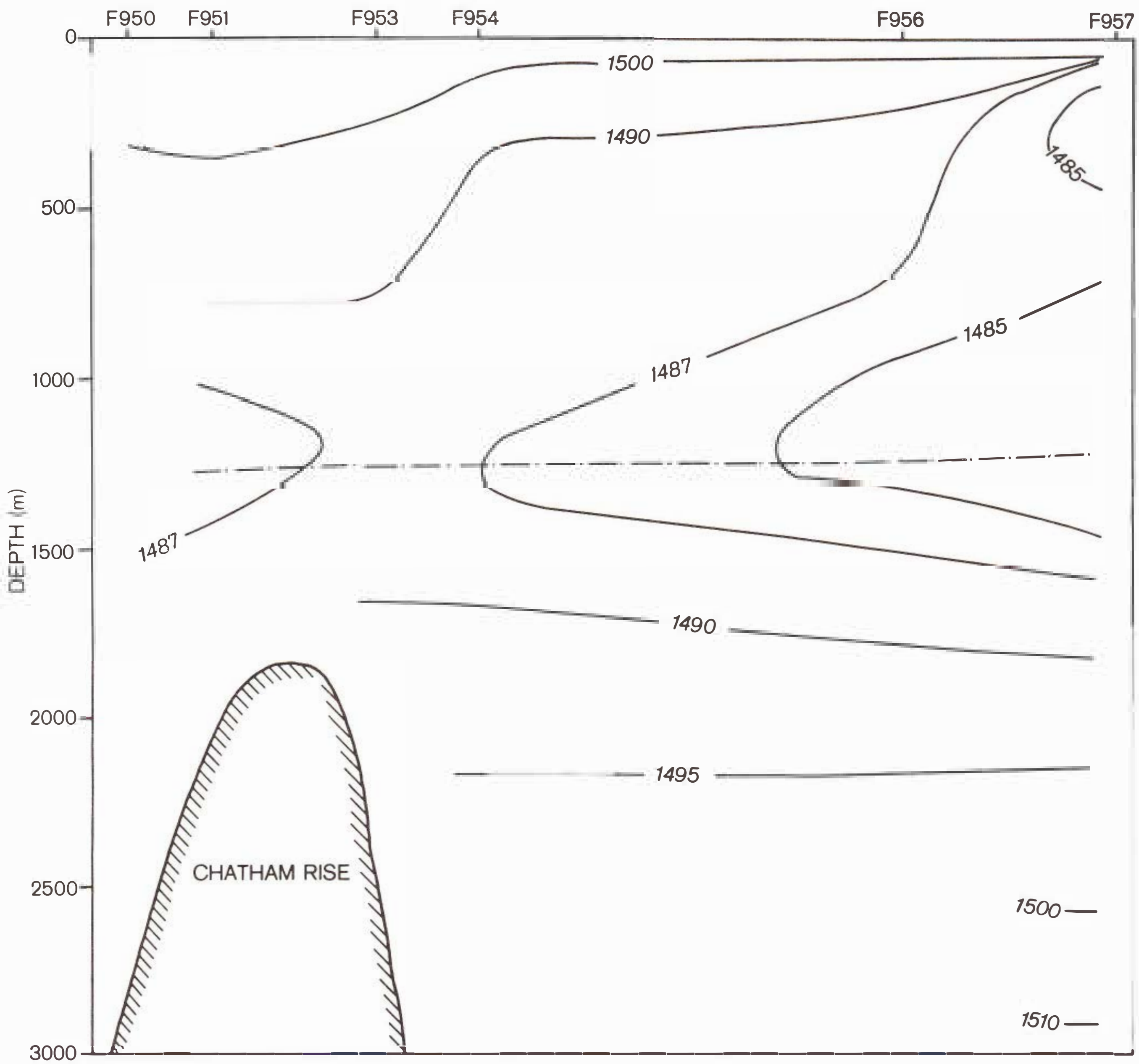

Fig. 15. Vertical cross-section of sound velocity (m sec^{-1}) along approximate longitude 174°W. Station numbers are shown.

ACKNOWLEDGMENTS

Assistance in field work by Messrs D.G. McKnight, W.deL. Main, N.H. Lambert, and B.S. Shakespeare (all of the N.Z. Oceanographic Institute) and by the officers and crew of MV *Taranui* commanded by the late Capt. D.K. Matheson is gratefully acknowledged. Thanks are expressed to the Applied Mathematics Division, DSIR, Wellington, for computing facilities; to Miss P. Lawrence, who prepared the drawings for publication; and to Mrs R.M.C. Thompson, who typed the manuscript.

Particular acknowledgment is made to the writer's former colleague, Dr D.M. Garner, who originally conceived the idea of carrying out the series of block surveys and who was responsible for the first four of these.

REFERENCES

BURLING, R.W. 1961: Hydrology of Circumpolar Waters south of New Zealand. *Mem. N.Z. oceanogr. Inst. 10. (Bull. N.Z. Dep. scient. ind. Res. 143.)* 65 p.

DEACON, G.E.R. 1937: The hydrology of the Southern Ocean. *'Discovery' Rep. 15* : 1-123.

GARNER, D.M. 1959: The Subtropical Convergence in New Zealand surface waters. *N.Z. Jl Geol. Geophys. 2(2)* : 315-37.

GARNER, D.M. 1967a: Hydrology of the Southern Hikurangi Trench Region. *Mem. N.Z. oceanogr. Inst. 39. (Bull. N.Z. Dep. scient. ind. Res. 177.)* 36 p.

GARNER, D.M. 1967b: Hydrology of the Southeast Tasman Sea. *Mem. N.Z. oceanogr. Inst. 48. (Bull. N.Z. Dep. scient. ind. Res. 181.)* 40 p.

GARNER, D.M. 1967c: Oceanic sound channels around New Zealand. *N.Z. Jl mar. Freshwat. Res. 1* : 3-15.

GARNER, D.M. 1969: The geopotential topography of the ocean surface around New Zealand. *N.Z. Jl mar. Freshwat. Res. 3(2)* : 209-19.

GARNER, D.M. 1970: Hydrological studies in the New Zealand region 1966 and 1967. *Mem. N.Z. oceanogr. Inst. 58. (Bull. N.Z. Dep. scient. ind. Res. 202.)* 51p.

HEATH, R.A. 1972: Choice of reference surface for geostrophic currents around New Zealand. *N.Z. Jl mar. Freshwat. Res. 6(1&2)* : 148-77.

HEATH, R.A. 1975: Oceanic circulation off the east coast of New Zealand. *Mem. N.Z. oceanogr. Inst. 55.*

MATTHEWS, D.J. 1939: Tables of the Velocity of Sound in Pure Water and Sea Water for use in Echo Sounding and Sound Ranging. *Publs Admty hydrogr. Dept. 282* : 1-52.

NEUMANN, G.; PIERSON, W.J.,Jr 1966: "Principles of Physical Oceanography". Prentice-Hall, Engelwood Cliffs, New Jersey. 545p.

RIDGWAY, N.M. 1970: Hydrology of the Southern Kermadec Trench Region. *Mem. N.Z. oceanogr. Inst. 56. (Bull. N.Z. Dep. scient. ind. Res. 205.)* 30p.

RIDGWAY, N.M.; HEATH, R.A. 1975: Hydrology of the Kermadec Islands Region. *Mem. N.Z. oceanogr. Inst. 73.* 28p.

WILSON, W.D. 1960: Speed of sound in sea-water as a function of temperature, pressure and salinity. *J. acoust. Soc. Am. 32(6)* : 641-4.

APPENDIX

NUMERICAL STATION DATA

D is the thermometrically measured pressure in decibars at each sampling point. This is numerically nearly equal to the geometric depths in metres. A more accurate conversion using representative mean density figures (LaFond 1951, p.8) is as follows:-

pressure (decibars) =	200	400	600	800	1000	1500	2000	2500
depth (metres)	199	398	595	793	991	1484	1976	2467

T is the sample temperature in °C x 100.

S is the sample salinity in ‰ x 100.

σ_t is the water density reduced to surface pressure isothermally x 100.

σ_{stp} is the *in situ* water density. The "σ" value is derived from the density, ρ, from the relationship $\sigma = (\rho-1) \times 10^5$ where ρ is the water density in g cm^{-3}.

ΣΔD is the cumulative anomaly of the geopotential distance between the sea surface and the sample depth in dynamic centimetres.

C is the *in situ* sound velocity in m s^{-1} x 10.

Cm is the integral mean sound velocity between the sea surface and the sample depth in m s^{-1} x 10.

K is the correction, in metres x 10, to be applied to an echo sounding of a depth corresponding to the depth D on a machine calibrated for a velocity of 1,500 m s^{-1}.

$\Sigma\Delta X = \int_p^0 \delta\, dp$ is the potential energy anomaly from the sea surface to the sample depth in kg m s^{-4} x 10^3 (p is the pressure and δ the specific volume anomaly giving the difference between the actual specific volume and that in a standard ocean at temperature 0°C and salinity at 35‰).

D	T	S	σ_t	σ_{stp}	ΣΔD	C	C_m	K	ΣΔX
F948									
0	1841	3552	2559	2559	0.0	15183	15183	0	0.0
23	1833	3546	2556	2566	5.5	15183	15183	3	64.1
45	1588	3538	2609	2629	10.4	15114	15166	5	228.3
68	1534	3544	2625	2656	14.7	15104	15146	7	471.6
90	1521	3544	2628	2668	18.6	15100	15135	8	781.8
135	1454	3534	2635	2695	26.5	15086	15121	11	1666.4
179	1372	3524	2645	2725	33.8	15064	15110	13	2826.9
357	1133	3499	2673	2833	61.0	15009	15073	17	10114.5
447	1028	3485	2681	2882	73.5	14985	15058	17	15129.8
556	929	3473	2688	2939	88.0	14965	15042	15	22402.9
700	781	3459	2700	3017	106.1	14930	15022	10	33752.7
803	700	3452	2706	3070	118.3	14915	15009	5	42898.7
879	654	3450	2711	3110	126.9	14910	15001	1	50180.0
1135	494	3448	2729	3246	153.6	14887	14978	-17	77006.4
1438	378	3450	2743	3399	180.9	14889	14959	-40	112157.7
F949									
0	1871	3529	2534	2534	0.0	15189	15189	0	0.0
22	1837	3530	2543	2553	5.7	15182	15186	3	63.0
46	1480	3517	2616	2637	11.0	15078	15156	5	244.2
67	1372	3517	2640	2670	14.7	15046	15127	6	453.7
90	1335	3522	2651	2691	18.4	15037	15105	6	743.9
134	1308	3519	2654	2714	25.2	15036	15082	7	1506.1
178	1270	3513	2657	2737	32.0	15029	15070	8	2555.4
266	1174	3500	2666	2785	45.1	15009	15053	9	5466.1
354	1081	3489	2674	2834	57.6	14989	15040	9	9361.2
460	960	3475	2684	2892	72.0	14961	15025	8	15216.6
528	885	3464	2688	2927	80.9	14943	15015	5	19603.2
658	791	3454	2695	2993	97.4	14927	14999	-0	29403.4
786	717	3450	2702	3058	113.1	14919	14987	-7	40694.6
958	630	3447	2712	3146	113.0	14913	14974	-17	58084.1
1088	530	3446	2723	3218	146.9	14893	14965	-25	72318.2
1298	403	3450	2741	3333	166.5	14875	14952	-41	95728.1
1505	324	3455	2753	3440	183.1	14879	14942	-58	118915.1
2134	209	3466	2771	3743	225.6	14935	14932	-97	196318.7
F950									
0	1812	3516	2538	2538	0.0	15170	15170	0	0.0
6	1812	3516	2538	2541	1.5	15172	15171	1	4.6
18	1456	3520	2624	2632	4.2	15065	15136	2	36.3

D	T	S	σ_t	σ_{stp}	ΣΔD	C	C_m	K	ΣΔX
F950 continued									
24	1389	3521	2639	2650	5.2	15044	15116	2	58.0
36	1375	3521	2642	2658	7.2	15043	15091	2	117.0
72	1358	3519	2644	2676	13.0	15041	15067	3	432.4
96	1337	3518	2648	2691	16.8	15039	15060	4	755.9
120	1291	3516	2655	2709	20.6	15027	15055	4	1159.4
144	1265	3512	2657	2722	24.2	15022	15050	5	1639.6
180	1203	3504	2663	2744	29.6	15005	15042	5	2505.6
216	1139	3498	2671	2768	34.7	14988	15035	5	3524.5
264	1057	3487	2677	2796	41.3	14966	15024	4	5105.4
F951									
0	1761	3500	2539	2539	0.0	15153	15153	0	0.0
12	1748	3500	2542	2547	3.1	15151	15152	1	18.6
26	1571	3498	2582	2593	6.4	15101	15138	2	82.0
40	1350	3497	2629	2647	9.2	15031	15113	3	173.3
82	1249	3500	2651	2688	16.1	15004	15064	3	596.8
168	1171	3498	2665	2740	29.0	14991	15030	3	2206.0
217	1105	3490	2671	2769	35.9	14975	15019	3	3545.4
273	1059	3486	2676	2799	43.7	14968	15010	2	5436.4
402	923	3468	2685	2867	60.8	14937	14991	-2	11217.7
490	865	3462	2690	2911	72.1	14929	14981	-6	16249.0
600	810	3457	2694	2966	85.9	14925	14971	-12	23776.4
665	750	3454	2701	3002	93.8	14913	14966	-15	28775.3
1099	459	3448	2733	3235	139.3	14866	14935	-47	68894.7
1315	366	3453	2747	3348	157.5	14964	14924	-67	90963.1
F952									
0	1737	3504	2547	2547	0.0	15147	15147	0	0.0
19	1733	3504	2548	2557	4.7	15149	15148	2	45.3
37	1384	3503	2626	2643	8.6	15043	15123	3	153.4
55	1314	3501	2639	2664	11.7	15023	15093	3	295.7
73	1283	3500	2645	2677	14.6	15014	15075	4	484.2
109	1226	3497	2653	2702	20.3	15001	15052	4	1000.0
215	1129	3491	2667	2764	36.0	14984	15023	3	3548.3
293	1049	3483	2675	2807	46.9	14967	15010	2	6322.9
355	997	3477	2680	2840	55.3	14957	15002	0	9044.9
531	862	3462	2690	2930	78.3	14934	14983	-6	19230.2
637	774	3455	2698	2987	91.5	14917	14974	-11	26916.8
777	679	3450	2707	3060	107.9	14902	14962	-20	38535.8
885	602	3447	2715	3118	119.9	14889	14954	-27	48439.3
1062	443	3448	2735	3221	137.1	14853	14940	-43	65251.7

F953

D	T	S	σ_t	σ_{stp}	ΣΔD	C	C_m	K	ΣΔX
0	1733	3500	2545	2545	0.0	15145	15145	0	0.0
46	1351	3491	2624	2644	9.9	15032	15089	3	229.4
68	1255	3492	2644	2674	13.7	15004	15066	3	443.8
91	1226	3494	2651	2692	17.3	14997	15049	3	733.7
137	1172	3495	2662	2724	24.3	14987	15030	3	1523.8
182	1124	3491	2668	2750	30.7	14977	15018	2	2555.1
364	883	3465	2689	2854	54.9	14915	14982	-4	9163.8
455	839	3459	2691	2898	66.3	14912	14968	-10	13799.2
546	784	3454	2696	2943	77.4	14907	14958	-15	19393.0
683	720	3449	2700	3010	93.9	14903	14948	-24	29524.8
849	636	3442	2707	3093	113.4	14897	14938	-35	44412.2
1001	566	3441	2715	3170	130.4	14893	14932	-46	60135.5
1138	483	3444	2727	3246	144.5	14882	14926	-56	75256.7
1894	256	3462	2764	3628	206.5	14914	14915	-107	169247.2
2296	209	3470	2775	3817	231.9	14962	14949	-124	222484.4

F954

D	T	S	σ_t	σ_{stp}	ΣΔD	C	C_m	K	ΣΔX
0	1633	3478	2552	2552	0.0	15113	15113	0	0.0
21	1623	3474	2551	2561	5.2	15112	15112	2	54.6
42	1282	3476	2626	2645	9.6	15006	15086	2	195.6
63	1186	3473	2643	2671	13.2	14976	15054	2	383.4
85	1102	3476	2660	2699	16.6	14952	15031	2	634.9
127	1048	3475	2669	2727	22.6	14939	15002	0	1269.3
235	930	3472	2687	2803	39.4	14916	14965	-6	4486.5
348	840	3461	2693	2851	50.8	14897	14949	-12	7921.6
443	778	3452	2695	2896	62.3	14886	14937	-19	12439.3
510	745	3449	2697	2929	70.2	14884	14930	-24	16247.5
612	708	3445	2700	2978	82.3	14886	14922	-32	23027.1
775	647	3441	2705	3057	101.4	14888	14915	-44	36258.0
926	566	3439	2713	3135	118.4	14881	14910	-56	50682.8
1079	489	3440	2723	3215	134.4	14874	14905	-68	66735.5
1295	400	3443	2735	3327	155.0	14873	14900	-86	91172.2
1579	332	3450	2748	3468	179.2	14893	14897	-108	126014.2
1724	296	3455	2755	3541	190.4	14903	14897	-118	144565.3
2068	230	3466	2770	3711	214.0	14933	14901	-137	189190.5
2467	204	3472	2777	3894	238.5	14990	14910	-147	244840.0

F956

D	T	S	σ_t	σ_{stp}	ΣΔD	C	C_m	K	ΣΔX
0	1469	3443	2562	2562	0.0	15057	15057	0	0.0
13	1461	3447	2567	2573	3.0	15056	15057	0	19.9
20	1271	3462	2618	2627	4.5	14997	15046	1	44.1
28	1164	3478	2651	2663	5.8	14964	15028	1	76.7
40	1130	3475	2655	2673	7.7	14954	15007	0	138.9
76	1098	3474	2660	2694	13.0	14948	14980	-1	449.6
110	1051	3475	2669	2719	17.9	14937	14969	-2	901.2
179	969	3470	2679	2760	27.2	14917	14935	-6	2244.1
203	914	3460	2680	2772	30.3	14901	14947	-7	2840.5
257	885	3461	2686	2802	37.2	14898	14937	-11	4425.7
346	805	3451	2690	2848	48.2	14881	14925	-17	7766.6
492	746	3444	2694	2917	66.1	14881	14912	-29	15246.5
569	708	3441	2696	2955	75.5	14879	14907	-35	20202.0
674	666	3439	2701	3007	88.0	14879	14903	-44	27983.0
847	559	3435	2711	3098	107.7	14863	14897	-58	42948.8
1019	451	3433	2722	3188	125.7	14848	14890	-75	59742.0
1190	371	3434	2731	3276	142.0	14842	14883	-93	77827.4
1565	284	3447	2750	3466	173.6	14870	14887	-129	121290.2
1878	251	3458	2762	3618	196.3	14910	14879	-152	160387.5
2220	240	3465	2768	3776	219.5	14963	14888	-166	207882.1

F957

D	T	S	σ_t	σ_{stp}	ΣΔD	C	C_m	K	ΣΔX
0	1319	3441	2592	2592	0.0	15008	15008	0	0.0
23	1318	3439	2590	2601	4.8	15010	15009	0	55.6

F958 continued

D	T	S	σ_t	σ_{stp}	ΣΔD	C	C_m	K	ΣΔX
46	1309	3439	2592	2613	9.6	15012	15010	0	222.9
69	948	3430	2651	2683	13.8	14887	14990	-0	464.0
92	849	3432	2669	2711	17.2	14853	14960	-2	734.9
137	795	3431	2676	2739	23.3	14841	14923	-7	1431.1
182	767	3431	2680	2763	29.1	14838	14902	-12	2367.3
364	714	3438	2693	2859	51.8	14847	14872	-31	8539.7
458	689	3436	2695	2904	63.0	14853	14867	-40	13156.0
551	682	3435	2695	2946	74.2	14864	14866	-49	18792.8
693	591	3432	2705	3021	90.8	14852	14864	-63	29135.2
834	497	3430	2715	3096	106.2	14836	14861	-77	40880.0
1023	400	3430	2725	3194	125.1	14826	14855	-99	58487.4
1166	333	3435	2736	3271	138.1	14823	14852	-115	72714.4
1406	289	3444	2747	3392	157.7	14846	14849	-142	97900.8
1645	267	3453	2756	3509	175.4	14877	14850	-164	124921.5
1885	248	3461	2764	3624	191.9	14909	14856	-181	153929.8
2369	220	3471	2774	3848	222.8	14980	14874	-199	219783.9
2854	184	3473	2779	4065	253.2	15046	14897	-195	299120.7
3343	154	3472	2780	4277	285.3	15116	14924	-169	398661.4

F958

D	T	S	σ_t	σ_{stp}	ΣΔD	C	C_m	K	ΣΔX
0	1436	3428	2557	2557	0.0	15045	15045	0	0.0
20	1428	3426	2558	2567	4.8	15045	15045	1	48.4
39	1306	3437	2591	2609	9.1	15009	15036	1	175.5
57	1012	3439	2648	2673	12.4	14910	15012	0	334.8
76	989	3442	2654	2688	15.4	14905	14986	-1	530.6
114	955	3457	2671	2723	20.9	14901	14958	-3	1051.6
151	882	3455	2681	2750	25.7	14878	14941	-6	1698.3
224	782	3445	2689	2791	34.8	14852	14916	-12	3400.3
300	749	3443	2692	2829	44.0	14852	14900	-20	5799.4
376	696	3441	2698	2870	52.9	14842	14889	-28	8813.4
602	554	3433	2710	2986	77.9	14821	14867	-53	21035.0
764	460	3431	2720	3070	94.4	14809	14856	-73	32349.4
888	389	3437	2732	3140	105.9	14802	14849	-89	41853.6
1090	312	3438	2740	3242	122.9	14801	14840	-116	58574.2
1295	289	3451	2753	3348	138.3	14827	14836	-141	76977.5
1500	265	3455	2758	3446	152.4	14852	14837	-163	96678.1
1938	227	3466	2770	3655	180.3	14910	14847	-198	144621.3
2378	206	3472	2776	3855	206.6	14976	14864	-215	201378.4
2863	177	3474	2780	4071	235.9	15045	14889	-212	278266.9

F959

D	T	S	σ_t	σ_{stp}	ΣΔD	C	C_m	K	ΣΔX
0	1377	3426	2568	2568	0.0	15025	15025	0	0.0
22	1298	3424	2583	2593	4.9	15002	15013	0	54.4
43	1055	3425	2629	2649	9.0	14920	14988	-0	188.7
69	903	3427	2656	2688	13.3	14870	14953	-2	424.9
93	811	3431	2674	2716	16.7	14840	14927	-4	700.1
140	779	3438	2684	2748	22.7	14835	14897	-10	1406.4
187	772	3443	2689	2774	28.5	14841	14882	-15	2348.8
281	716	3443	2697	2825	39.5	14836	14868	-25	4936.8
370	664	3438	2700	2869	49.7	14829	14859	-35	8231.2
461	628	3435	2702	2914	59.9	14829	14853	-45	12479.3
597	578	3432	2706	2980	75.0	14830	14848	-61	20456.0
732	471	3430	2718	3054	89.1	14809	14843	-77	29871.2
912	369	3432	2730	3150	106.1	14796	14835	-101	43852.9
1040	326	3436	2737	3216	117.1	14799	14830	-118	54575.1
1259	294	3445	2747	3326	134.4	14824	14827	-145	74427.8
1478	265	3454	2757	3435	150.0	14848	14828	-169	95810.0
1695	250	3461	2764	3540	164.2	14879	14833	-189	118378.5
2129	213	3471	2775	3745	190.4	14936	14848	-216	168471.4
2570	179	3473	2779	3944	215.8	14996	14868	-226	228112.4
3036	150	3473	2782	4149	243.6	15063	14893	-217	305868.8

F960

D	T	S	σ_t	σ_{stp}	ΣΔD	C	C_m	K	ΣΔX
0	1546	3446	2547	2547	0.0	15082	15082	0	0.0
19	1538	3444	2548	2556	4.7	15082	15082	1	45.4
34	1028	3444	2649	2664	7.8	14913	15045	1	126.5
50	954	3447	2664	2686	10.2	14888	14998	-0	226.8
67	946	3448	2666	2696	12.6	14889	14970	-1	367.5
98	913	3454	2676	2720	16.8	14882	14943	-4	715.9
130	888	3453	2679	2738	21.0	14877	14927	-6	1192.1
192	865	3452	2682	2769	29.0	14880	14912	-11	2475.3
255	802	3446	2687	2803	36.9	14864	14902	-17	4249.2
318	787	3445	2688	2833	44.7	14868	14895	-22	6488.1
380	768	3443	2689	2862	52.4	14872	14891	-28	9169.4
474	730	3441	2693	2909	63.9	14871	14887	-36	14099.1
565	697	3439	2696	2954	75.0	14874	14885	-43	19820.4
694	616	3434	2703	3020	90.1	14862	14881	-55	29381.9
790	531	3432	2712	3073	100.8	14844	14878	-64	37297.0
946	413	3432	2725	3160	116.5	14821	14870	-82	50955.2

F961

D	T	S	σ_t	σ_{stp}	ΣΔD	C	C_m	K	ΣΔX
0	1488	3434	2551	2551	0.0	15062	15062	0	0.0
24	1417	3437	2568	2579	5.7	15043	15052	1	69.2
48	1128	3440	2628	2649	10.6	14950	15024	1	245.7
72	935	3444	2664	2697	14.4	14884	14988	-1	475.0
95	911	3447	2671	2714	17.6	14880	14962	-2	742.6
190	860	3453	2683	2770	30.1	14876	14920	-10	2521.6
285	799	3448	2689	2819	42.0	14868	14904	-18	5331.6
379	767	3444	2690	2863	53.5	14871	14896	-26	9166.9
473	736	3442	2693	2909	65.0	14874	14891	-34	14068.8
568	697	3440	2697	2956	76.5	14874	14888	-42	20038.3
710	600	3434	2705	3029	93.0	14857	14884	-55	30605.2
852	518	3431	2713	3102	108.7	14848	14878	-69	42830.3

F962

D	T	S	σ_t	σ_{stp}	ΣΔD	C	C_m	K	ΣΔX
0	1546	3445	2547	2547	0.0	15082	15082	0	0.0
22	1479	3438	2556	2566	5.4	15063	15072	1	60.0
43	929	3435	2658	2678	9.5	14876	15022	1	193.6
65	856	3433	2668	2698	12.7	14853	14968	-1	362.9
87	816	3432	2674	2713	15.6	14841	14937	-4	589.8
130	796	3435	2679	2738	21.3	14840	14905	-8	1201.7
174	780	3440	2685	2765	26.8	14842	14889	-13	2047.3
260	768	3444	2690	2809	37.4	14853	14875	-22	4330.1
347	745	3441	2691	2849	47.9	14856	14870	-30	7527.8
434	709	3439	2695	2893	58.4	14856	14867	-38	11619.9
564	636	3435	2701	2959	73.6	14849	14864	-51	19218.1
695	514	3431	2713	3032	87.9	14820	14858	-66	28240.7
868	404	3431	2726	3125	105.0	14804	14849	-87	41575.0
998	356	3434	2733	3192	116.7	14805	14843	-104	52511.3
1215	305	3443	2745	3303	134.6	14820	14838	-131	72245.9
1430	271	3455	2757	3414	150.1	14843	14837	-156	92749.5

F963

D	T	S	σ_t	σ_{stp}	ΣΔD	C	C_m	K	ΣΔX
0	1393	3426	2565	2565	0.0	15030	15030	0	0.0
20	1356	3423	2570	2579	4.6	15021	15026	0	46.5
38	996	3417	2633	2650	8.2	14898	14994	-0	151.2
58	939	3417	2643	2669	11.5	14880	14958	-2	311.3
116	711	3421	2680	2733	20.0	14804	14900	-8	1042.3
309	648	3431	2697	2838	43.3	14812	14842	-33	6010.3
385	584	3426	2701	2878	51.9	14797	14835	-42	8996.9
502	570	3432	2707	2938	64.7	14811	14828	-58	14675.5
616	465	3429	2717	3001	76.5	14787	14822	-73	21225.3
765	369	3430	2728	3081	90.4	14771	14814	-95	30835.6

F962 continued

D	T	S	σ_t	σ_{stp}	ΣΔD	C	C_m	K	ΣΔX
1239	261	3452	2756	3327	126.9	14806	14804	-162	67435.2
1470	254	3458	2761	3437	141.8	14842	14807	-189	87582.7
1784	229	3467	2771	3587	160.7	14885	14817	-217	118395.2
2147	213	3471	2775	3753	181.6	14939	14833	-239	159423.4
2510	188	3473	2779	3916	202.6	14990	14852	-248	208329.5

F964

D	T	S	σ_t	σ_{stp}	ΣΔD	C	C_m	K	ΣΔX
0	1344	3415	2567	2567	0.0	15013	15013	0	0.0
25	1241	3425	2595	2606	5.5	14984	14998	-0	68.8
50	1108	3427	2621	2644	10.3	14941	14981	-1	251.5
75	858	3427	2663	2698	14.4	14855	14953	-2	505.9
99	799	3436	2679	2725	17.7	14836	14927	-5	788.9
199	691	3433	2692	2784	29.9	14810	14875	-17	2616.4
298	659	3431	2695	2832	41.5	14813	14854	-29	5486.7
397	613	3428	2699	2881	52.9	14812	14843	-41	9446.2
497	563	3427	2704	2932	64.1	14808	14837	-54	14454.4
646	475	3426	2714	3011	79.9	14796	14829	-74	23491.7
794	391	3429	2725	3091	94.3	14785	14821	-95	33848.8
993	328	3437	2738	3196	111.5	14792	14815	-123	49291.1
1241	273	3448	2752	3323	130.3	14812	14812	-155	70289.6
1490	262	3453	2757	3440	147.6	14849	14815	-184	93800.3

F965

D	T	S	σ_t	σ_{stp}	ΣΔD	C	C_m	K	ΣΔX
0	1166	3418	2604	2604	0.0	14953	14953	0	0.0
17	1138	3417	2608	2616	3.3	14946	14949	-1	28.3
36	1030	3418	2628	2644	6.8	14911	14938	-1	121.5
48	939	3418	2643	2665	8.8	14879	14927	-2	206.5
64	773	3421	2671	2701	11.2	14820	14908	-4	339.2
104	673	3429	2692	2740	16.2	14788	14868	-9	761.1
235	561	3421	2700	2808	31.0	14763	14816	-29	3274.3
392	481	3423	2711	2892	47.7	14756	14793	-54	8483.8
508	428	3425	2718	2953	59.1	14753	14785	-73	13626.3
624	377	3428	2726	3015	69.8	14752	14779	-92	19687.1
777	327	3433	2735	3094	82.9	14755	14774	-117	28841.9
886	292	3437	2741	3151	91.5	14759	14772	-135	36000.6
1057	274	3447	2751	3239	103.9	14781	14771	-161	48036.3
1232	255	3453	2757	3325	115.5	14803	14774	-185	61331.1
1384	253	3458	2761	3398	125.1	14827	14779	-204	73858.0
1677	235	3466	2769	3538	142.6	14870	14791	-234	100636.6
1887	212	3470	2774	3637	154.3	14896	14801	-250	121581.4
2099	204	3472	2777	3734	165.9	14928	14812	-263	144673.9

F966

D	T	S	σ_t	σ_{stp}	ΣΔD	C	C_m	K	ΣΔX
0	973	3417	2637	2637	0.0	14883	14883	0	0.0
22	953	3415	2639	2649	3.6	14879	14881	-2	40.1
45	921	3439	2663	2683	7.1	14875	14879	-4	158.8
67	802	3439	2681	2712	10.1	14833	14871	-6	324.4
90	795	3447	2689	2730	12.9	14835	14861	-8	545.4
135	767	3447	2693	2755	18.2	14832	14852	-13	1140.9
180	759	3447	2694	2776	23.4	14835	14847	-18	1962.4
254	731	3445	2696	2813	32.0	14837	14844	-26	3812.7
339	626	3429	2698	2854	41.7	14808	14839	-36	6694.6
424	557	3422	2701	2896	51.3	14792	14831	-48	10356.8
550	496	3422	2708	2961	65.0	14788	14821	-65	17051.3
677	450	3423	2714	3026	78.2	14790	14815	-83	25165.7
846	346	3430	2731	3121	94.2	14774	14809	-108	37323.2
971	322	3435	2737	3185	104.8	14786	14805	-126	46923.3
1183	292	3444	2747	3291	121.4	14810	14804	-155	64807.2
1394	269	3451	2754	3395	136.6	14835	14806	-180	84363.5
1607	258	3458	2761	3497	150.9	14867	14812	-201	105907.5
2045	235	3464	2768	3699	179.4	14932	14831	-231	157837.7

D	T	S	σ_t	σ_{stp}	ΣΔD	C	C_m	K	ΣΔX
F968									
0	1285	3432	2592	2592	0.0	14995	14995	0	0.0
24	1284	3430	2590	2601	5.0	14998	14996	-0	60.6
49	920	3431	2657	2679	9.5	14874	14965	-1	225.0
73	818	3433	2674	2708	12.9	14839	14929	-3	431.0
98	784	3436	2682	2726	16.1	14831	14905	-6	707.4
134	769	3442	2688	2750	20.5	14832	14885	-10	1221.0
177	749	3443	2692	2773	25.6	14831	14872	-15	2014.4
261	736	3444	2695	2814	35.5	14840	14860	-24	4162.7
344	689	3437	2696	2853	45.1	14834	14855	-33	7085.1
429	629	3430	2698	2895	55.0	14823	14849	-43	10891.2
554	554	3430	2708	2962	68.9	14814	14843	-58	17734.1
F969									
0	1427	3425	2557	2557	0.0	15041	15041	0	0.0
21	1421	3423	2557	2566	5.1	15042	15042	1	53.5
42	1286	3424	2585	2604	9.9	15001	15032	1	205.7
63	1046	3425	2631	2659	14.0	14920	15008	0	421.0
84	937	3424	2648	2687	17.5	14885	14981	-1	676.7
95	838	3429	2668	2711	19.1	14850	14968	-2	822.6
128	793	3432	2677	2736	23.5	14838	14936	-5	1318.8
191	776	3441	2687	2774	31.5	14844	14905	-12	2593.1
253	760	3445	2692	2808	39.0	14848	14890	-18	4256.0
312	740	3442	2693	2835	46.0	14850	14882	-24	6239.9
398	701	3439	2696	2878	56.2	14848	14875	-33	9857.2
472	642	3435	2701	2917	64.8	14836	14870	-41	13585.0
580	566	3433	2709	2975	76.7	14823	14862	-53	19868.5
664	509	3432	2715	3019	85.5	14814	14857	-63	25339.8
803	425	3432	2724	3093	99.2	14801	14848	-81	35340.2
939	359	3434	2732	3165	111.5	14797	14841	-99	46040.8
1080	332	3439	2739	3236	123.3	14808	14836	-118	58018.2
1356	273	3452	2755	3378	144.0	14830	14833	-151	83254.5
F970									
0	1479	3427	2547	2547	0.0	15058	15058	0	0.0
21	1477	3425	2546	2556	5.3	15061	15059	1	55.6
41	905	3423	2653	2671	9.3	14865	15012	0	181.3
61	841	3426	2665	2693	12.2	14845	14960	-2	330.9
82	791	3426	2673	2710	15.1	14829	14928	-4	537.3
131	758	3430	2681	2741	21.5	14825	14890	-10	1219.6
164	774	3440	2686	2761	25.7	14839	14878	-13	1828.5
260	754	3442	2691	2809	37.3	14847	14865	-23	4302.1
346	713	3438	2693	2851	47.6	14843	14860	-32	7421.5
429	657	3435	2699	2895	57.3	14835	14856	-41	11189.6
556	559	3432	2709	2964	71.4	14816	14849	-56	18130.0
680	468	3430	2718	3030	84.2	14798	14842	-72	26007.9
870	390	3431	2727	3127	102.3	14798	14832	-97	40030.4
977	331	3434	2735	3185	111.7	14791	14828	-112	48703.5
1190	296	3442	2745	3292	128.8	14811	14823	-140	67234.8
1402	270	3452	2755	3399	144.2	14837	14823	-165	87209.6
1614	259	3459	2762	3501	158.4	14869	14827	-186	108585.8
1984	223	3467	2771	3676	181.4	14915	14839	-213	150024.2
F971									
0	1489	3437	2553	2553	0.0	15063	15063	0	0.0
21	1485	3436	2553	2562	5.1	15064	15064	1	54.3
42	1350	3442	2586	2605	10.0	15024	15054	2	207.4
64	941	3447	2666	2695	13.9	14887	15020	1	415.2
84	905	3449	2673	2711	16.7	14877	14987	-1	618.3
121	899	3448	2673	2728	21.6	14879	14953	-4	1127.3
157	871	3454	2682	2754	26.3	14876	14936	-7	1780.4
226	819	3448	2686	2789	35.0	14866	14916	-13	3439.4
294	779	3444	2689	2823	43.4	14862	14904	-19	5628.4
365	750	3442	2691	2858	52.1	14861	14896	-25	8491.7
467	742	3439	2690	2903	64.7	14876	14890	-34	13723.0
569	638	3436	2702	2962	76.9	14850	14885	-44	20043.1
705	551	3432	2710	3032	92.0	14837	14877	-58	29685.2
808	484	3430	2716	3086	102.9	14826	14871	-69	37907.3
978	452	3432	2721	3169	120.1	14842	14865	-88	53305.7
F972									
0	1391	3437	2574	2574	0.0	15031	15031	0	0.0
23	1390	3434	2572	2582	5.2	15033	15032	0	60.2
45	1112	3441	2631	2652	9.6	14944	15011	0	210.5
68	992	3457	2665	2696	13.2	14907	14982	-1	414.7
91	927	3455	2674	2716	16.4	14866	14960	-2	665.6
138	873	3452	2681	2743	22.5	14873	14933	-6	1367.8
183	847	3449	2682	2766	28.3	14871	14918	-10	2288.9
275	811	3447	2686	2811	39.9	15871	14902	-18	4946.3
367	793	3446	2688	2855	51.4	14879	14895	-26	8640.7
461	779	3445	2689	2899	63.1	14889	14893	-33	13519.3
556	773	3444	2689	2942	75.2	14903	14893	-40	19633.7
650	718	3440	2694	2989	87.0	14895	14894	-46	26768.8
697	690	3437	2696	3012	92.8	14892	14894	-49	30688.9